# A research and production geothermal project on the TU Delft campus initial modeling and establishment of a digital twin

Voskov, Denis; Abels, Hemmo; Barnhoorn, Auke; Chen, Yuan; Daniilidis, Alexandros; Bruhn, David; Drijkoningen, Guy; Geiger, Sebastian; Laumann, Susanne; Song, Guofeng

**Publication date**
2024

**Document Version**
Final published version

**Published in**
PROCEEDINGS, 49th Workshop on Geothermal Reservoir Engineering

**Citation (APA)**
Voskov, D., Abels, H., Barnhoorn, A., Chen, Y., Daniilidis, A., Bruhn, D., Drijkoningen, G., Geiger, S., Laumann, S., Song, G., Vardon, P. J., Vargas Meleza, L., Verschuur, E., & Vondrak, A. (2024). A research and production geothermal project on the TU Delft campus: initial modeling and establishment of a digital twin. In *PROCEEDINGS, 49th Workshop on Geothermal Reservoir Engineering* Stanford University. https://pangea.stanford.edu/ERE/db/GeoConf/papers/SGW/2024/Voskov.pdf

PROCEEDINGS, 49th Workshop on Geothermal Reservoir Engineering
Stanford University, Stanford, California, February 12-14, 2024
SGP-TR-227

# A research and production geothermal project on the TU Delft campus: initial modeling and establishment of a digital twin

Denis VOSKOV[1,2], Hemmo ABELS[1], Auke BARNHOORN[1], Yuan CHEN[1], Alexandros DANIILIDIS[1], David BRUHN[1,3], Guy DRIJKONINGEN[1], Sebastian GEIGER[1], Susanne LAUMANN[1], Guofeng SONG[1], Philip J. VARDON[1], Liliana VARGAS MELEZA[1], Eric VERSCHUUR[1], and Andrea VONDRAK[1]

[1]Department of Geoscience & Engineering, TU Delft, Stevinweg 1, 2628 CN Delft, Netherlands

[2]Department of Energy Science & Engineering, Stanford University, Stanford, CA 94305, USA

[3]Fraunhofer Institution for Energy Infrastructures and Geothermal Systems IEG, Gulbener Str.23, 03046 Cottbus, Germany

D.V.Voskov@tudelft.nl

**Keywords:** geothermal doublet, direct-use heating, digital twin, uncertainty quantification, water loss

**ABSTRACT**

Nearly half of the Netherlands' natural gas consumption is allocated to heating, with direct-use geothermal heating being one of the available low-carbon energy solutions. A geothermal well doublet, designed with the two primary aims of research and commercial heat supply, is currently being installed on the campus of Delft University of Technology. The project is a key national research infrastructure and is being incorporated into the European sustainable and distributed infrastructure (EPOS: European Plate Observing System, https://www.epos-eu.org/), such that accessibility and data availability will be as wide as possible. All observations will be included in a digital-twin framework, which will allow us to make better decisions in future geothermal projects. The project includes a comprehensive research program, involving the installation of a wide range of instruments alongside an extensive logging and coring program and monitoring network. The doublet has been cored, with substantial continuous samples from the heterogeneous reservoir, alongside a large suite of well logs in both the reservoir and overlying geological units. Such investigation is rarely undertaken in geothermal projects. A fiber-optic cable will monitor the producer well all the way down to the reservoir section, at approximately 2300m depth, in the Lower Cretaceous Delft Sandstone that is used as a geothermal reservoir in a series of existing and planned doublets in the West Netherlands Basin. A local seismic monitoring network has been installed in the surrounding area with the aim of monitoring very low-magnitude natural or induced seismicity. A vertical observation well with electromagnetic sensors will be drilled in the near future between the injector and producer to monitor cold-front propagation. This paper presents the initial modeling for the project and steps towards the production of a digital twin. Two modeling examples in the paper will emphasize current operational challenges relevant to the project.

## 1. INTRODUCTION

Direct-use geothermal heating offers a clean baseload alternative to fossil fuels for the provision of space heating (Anderson & Rezaie, 2019; Lund & Toth, 2021). In low-enthalpy direct-use geothermal systems, hot water (or another working fluid) is extracted from the reservoir and usually reinjected back into the same reservoir after the extraction of thermal energy from the working fluid. The low-enthalpy direct-use geothermal project on the campus of the Delft University of Technology (with the name "Geothermie Delft") has been initiated to provide a unique research environment, alongside commercial thermal energy production, with the vision to scale up the deployment of geothermal energy as well as provide heating for the TU Delft campus and part of the city of Delft (Bruhn et al., 2015; P. Vardon et al., 2020). A geothermal doublet has been successfully installed on the TU Delft campus during the second half of 2023, with initial energy production planned for 2025. The total project is targeted to supply around 25 MW of thermal energy at peak conditions, and a thermal energy storage system is currently being developed to provide a seasonal buffer.

The research questions that are targeted to be answered relate to field-scale geothermal operations, e.g., how reliable is the long-term energy production, how do materials perform in the long term, and how geothermal projects can be best monitored. The project incorporates a comprehensive research program, deploying various instruments, extensive logging and coring programs, and a monitoring network (P. J. Vardon et al., 2024). Despite these rare extensive data collection initiatives, the inherent complexity of geological uncertainty and limited spatial data away from the wells necessitate computer models to gain comprehensive system understanding. Advancements in information technologies and associated hardware now enable improved data collection, transmission, and processing.

A digital twin denotes a virtual representation of a physical product, process, or facility, and is used to record, understand and predict the physical counterpart (Chen, 2017; Glaessgen & Stargel, 2012; Grieves, 2014). It divides the system into three components: a physical entity, a digital counterpart, and the connection linking the physical and digital parts. The digital model is consistently updated with current operating data from the physical part. The model's outputs, such as optimal operation strategies, can then be continually fed back to the physical entity. Real-time monitoring and prediction of events within a digital twin system can lead to cost reduction, improved efficiency, and risk mitigation (Yu et al., 2022). The digital twin concept has gained increasing attention and has gradually found

applications in various industries. However, there is limited published research on its application in geothermal energy. Konstantopoulos et al. (2023) gave a geothermal operations optimization framework based on machine learning (GOOML). With component modeling under constraints informed by physics, such a method is possible to be developed into a digital twin for the ground steam field using data collected from wells, pipelines, and power generation stations. Osinde et al. (2019) presented the design and implementation of a digital twin model of a geothermal drilling bit. By incorporating a torque sensor on the drill shaft and relaying this information to the digital twin, an accurate representation of the drill tip's status can be obtained. We proposed a digital twin for subsurface geothermal production that would help mitigate operational risks, reduce maintenance costs, extend reservoir longevity, and enhance the overall sustainability of a geothermal resource. To actualize this concept, the crucial elements lie in geological modeling, reservoir modeling coupled with uncertainty analysis, and data assimilation.

Geological modeling is essential for geothermal production to predict resource distribution and exploitation potential (Jolie et al., 2021). It is also the basis for informed optimization and decision-making in field operations. Current modeling tools often demand specialized knowledge to capture specific features of interest. They are usually time-consuming to create or revise the full extent of uncertainty and lack intuitiveness for non-specialists from different disciplines (Jacquemyn et al., 2023). Sketch-based interface and modeling (SBIM) is an approach for rapid model creation that has recently been used for prototyping in geological applications. It is based on the concept of using surfaces to capture geological architecture and heterogeneity (M. D. Jackson et al., 2009). Jacquemyn et al. (2021) showed SBIM to swiftly build 3D geological models of complex stratigraphy and structure. Their study highlights SBIM's efficiency in exploring various geological interpretations within hours, rather than days or weeks while maintaining fidelity to input data. The SBIM methods presented here are implemented in an open-source research code (Rapid Reservoir Modelling, RRM), which links a sketching interface with geological operators to build 3D models. A detailed introduction can be found in the section hereinafter. W. A. Jackson et al. (2022) and Alshakri et al. (2023) employed a combination of experimental design, sketch-based reservoir modeling, and flow diagnostics to swiftly assess the influence of sedimentological heterogeneities, acting as baffles and barriers, on $CO_2$ migration.

Geothermal energy production faces uncertainties. They stem from incomplete knowledge derived from underground reservoirs, which are limited by geological measurements and samples. For instance, relationships like permeability and porosity are often based on empirical correlations derived from data interpretation and core analysis (Chang et al., 1994; Willems et al., 2020). The physical and thermal attributes of both fluids and rocks, such as salinity, density, thermal capacity, and conductivity, can vary over geological timescales due to mineral dissolution and rock compositions. Additionally, corresponding geological interpretations are often not unique which exacerbates the overall uncertainty (Brunetti et al., 2019). A considerable degree of uncertainty is induced in reservoir modeling and characterization, commonly referred to as geological uncertainty (Yousefzadeh et al., 2023).

Macro-scale geological uncertainty extends to structure, reservoir architecture, continuity, and connectivity, leading to diverse geological concepts and scenarios. Despite previous research exploring geological scenarios, most reservoir modeling workflows are designed to explore and quantify uncertainty around a single geological concept or interpretation scenario (or hypothesis) using stochastic (probabilistic) modeling techniques (Linde et al., 2015; Refsgaard et al., 2012). However, to capture the full uncertainties within the system, it is necessary to explore uncertain geological model concepts and interpretation scenarios and quantify their impact on predicted behavior during the model prototyping stage (Bentley, 2016; Petrovskyy et al., 2023). Micro-scale uncertainty shows variations in geological properties such as permeability, porosity, thermal properties, fluid contacts, and characteristics of aquifers. These variations significantly influence energy quantities and heat transport mechanisms within the reservoir (Wang et al., 2023). Moreover, economic considerations play a vital role in the operation of a geothermal reservoir, directly impacting project feasibility and benefits (Daniilidis et al., 2021). Economic factors like heat and electricity prices are subject to market fluctuations, introducing uncertainties into the overall assessment of a geothermal project's viability (Daniilidis et al., 2017; De Paepe & Mertens, 2007). Full uncertainty evaluation often requires a significant number of forward evaluations, which is also challenged by the high resolution often required for such models (Athens & Caers, 2019; Wang et al., 2023).

To reduce uncertainties, models can be aligned with real-world observations such as well temperatures, flow rates, and, when possible, time-lapse data. This aligning process, known as history matching, involves tweaking uncertain geological model inputs and eliminating unfeasible model inputs such as the geological model, the permeability, porosity, and thermal conductivity to achieve a model response in line with observations. Various studies have highlighted this calibration technique for geothermal production (O'Sullivan & O'Sullivan, 2016; Rath et al., 2006; Tian et al., 2024; Wu et al., 2021; Zhang et al., 2014). Addressing geological uncertainties often involves adopting the Bayesian approach, integrating available prior knowledge like data from samples, geological formation scenarios, and assumptions about statistical distributions. The Bayesian method begins with prior information on model parameters and uses observed data (often with noise) to explore the relationship between observations and these parameters (Hoteit et al., 2012; Oliver et al., 2008). History matching, within this framework, aims to merge observed data with prior parameters to generate a revised estimate for the uncertain model.

The paper is structured as follows. We first introduce a digital twin framework for geothermal energy production, highlighting the key components that include the open-source geological modeling software RRM and the high-fidelity simulator DARTS. We then present two applications of our methods for addressing operational challenges at Delft campus geothermal wells. The first involves uncertainty analysis for bottom hole pressure (BHP) using realistic well log data, and the second analyzes the influence of a well side track on BHP and flow rate considering the open upper formation. In the final section, we summarize key conclusions and give our plans for a proof-of-concept study on a doublet system toward an open-source digital twin for subsurface geothermal systems.

## 2. METHODOLOGY

### 2.1 Digital Twin Framework for Geothermal Production

Here we propose a concept for a Digital Twin for Geothermal Energy that will be tested and validated at the geothermal project at TU Delft campus. Multiple geological models will be expeditiously constructed for the reservoir. The production data will be used for updating the geological models in real-time, constraining reservoir uncertainties, and adapting operational strategies to boost performance. Our workflow for an open-source digital twin for geothermal energy contains the following elements: a) Well logs and seismic data are utilized to design multiple reservoir models that capture possible geological scenarios, using the Rapid Reservoir Modeling (RRM) software; RRM is a sketch-based modeling software that allows users to rapidly sketch geologically consistent models in 3D. b) Possible property distributions will be assigned to geological domains to capture uncertainty in the petrophysical data. c) The reservoir simulator Delft Advanced Research Terra Simulator (DARTS) is combined with machine learning techniques to create proxy models that enable fast simulations. d) As new production and monitoring data becomes available, data assimilation techniques like Ensemble Smoother with Multiple Data Assimilation (ESMDA) are applied to update property distributions for each scenario. This iterative process of data assimilation will help users to constrain geological and production uncertainties, both of which are key to optimizing operational strategies. Overall, the geothermal digital twin is envisioned to decrease operational risks, reduce maintenance costs, extend reservoir lifetimes, and enhance the overall sustainability of geothermal resources.

### 2.2 Rapid Reservoir Modelling

Rapid Reservoir Modelling (RRM) is an open-source, sketch-based modeling tool with an intuitive interface enabling users to swiftly create 3D geologically consistent 3D reservoir models from 2D sketches (Jacquemyn et al., 2021; Petrovskyy et al., 2023). RRM integrates sketch-based interface and modeling (SBIM) with geological operators and near-real-time flow diagnostics. The combination of SBIM and geological operators allows users to build complex 3D geological models in a matter of minutes while flow diagnostics provide approximate information on the dynamic reservoir behavior within seconds. The latest releases of RRM can be downloaded from https://bitbucket.org/rapidreservoirmodelling/rrm/src/phase2/. RRM uses the concept of surface-based reservoir modeling (Jacquemyn et al., 2019), meaning that all geological architectures and heterogeneities are represented by surfaces that define enclosed volumes, the geological domains. These surfaces can represent a hierarchy of heterogeneities such as faults, stratigraphic surfaces, facies, or diagenetic bodies. Petrophysical properties such as are directly attributed to the geological domains, meaning that each domain has a constant property that is associated with a geologically meaningful volume. A grid is created in RRM on the fly and only when required for computations.

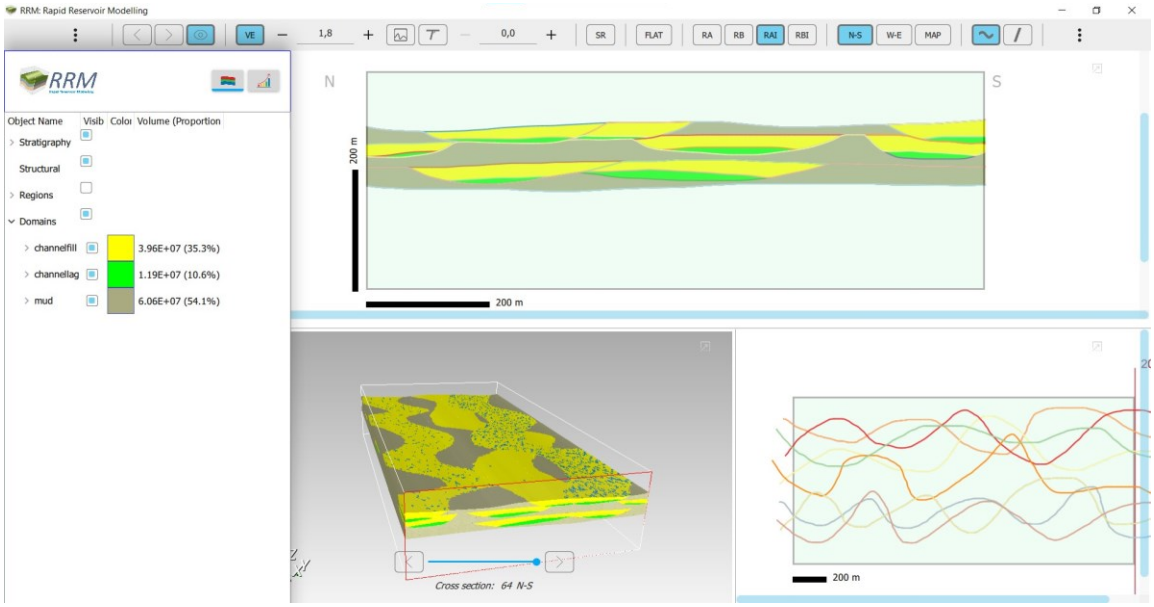


**Figure 1: Screenshot of the RRM interface, showing the cross-section sketching canvas (top right), map view sketching canvas (bottom right), 3D perspective view (bottom center), and a stratigraphic panel of sketched surfaces and domains. The sketched model corresponds to simple fluvial channelized deposits.**

Sketches drawn as 2D cross-sections and map views are integrated to form 3D bodies (fig. 1). There are three approaches to creating 3D volumes from 2D sketches (Jacquemyn et al., 2021). First, sketches from multiple vertical 2D cross-sections can be interpolated to create 3D surfaces. Second, contours sketched, for example, geological maps, can be interpolated in depth to create 3D surfaces. Third, the sketch of a vertical 2D cross-section can be extruded along a trajectory sketched in map view, indicating for example the shape of a fluvial channel, to create 3D surfaces. Geological operators within the modeling engine of RRM ensure that the 3D surfaces interact with each other in a geologically consistent way while providing the flexibility to "sketch as you see" (Jacquemyn et al., 2021). RRM is designed to be geologically intuitive and does not require specialist reservoir modeling experience. It allows users to quickly create, test, and explore geological concepts of reservoir architectures in data-poor environments or revise and update existing reservoir models. RRM applications include but are not limited to $CO_2$ storage (W. A. Jackson et al., 2022) and geothermal energy (Baird et al., 2023).

### 2.3 Delft Advanced Research Terra Simulator

The reservoir model should describe the porous media heat flow that can account for the transfer of heat between fluids and rock through convective and conductive fluxes. Within geothermal reservoir simulation, the governing equations include mass and energy conservation with closure assumptions on the thermal equilibrium between different phases including the solid. Typically, the fully coupled fully implicit scheme finds application in numerical geothermal simulations due to its unconditional stability. In this study, we utilize the Delft Advance Research Terra Simulator (DARTS) which embraced a fully-implicit solution employing the finite volume method alongside the two-point flux approximation to discretize these governing equations.

Conservation equations governing geothermal applications can be written in the following form:

$$\frac{\partial}{\partial t}\left(\phi \sum_{j=1}^{n_p} \rho_j s_j\right) - \nabla \cdot \sum_{j=1}^{n_j} \rho_j v_j + \sum_{j=1}^{n_p} \rho_j \tilde{q}_j = 0, \tag{1}$$

$$\frac{\partial}{\partial t}\left(\phi \sum_{j=1}^{n_p} \rho_j s_j U_j + (1-\phi) U_r\right) - \nabla \cdot \sum_{j=1}^{n_p} h_j \rho_j v_j + \nabla \cdot (\kappa \nabla T) + \sum_{j=1}^{n_p} h_j \rho_j \tilde{q}_j = 0, \tag{2}$$

where $t$ denotes time, $\phi$ the porosity of the media, $n_p$ the total number of phases existing in the geothermal system, $\rho_j$ the density of phase $j$, $s_j$ the saturation of phase $j$, $\tilde{q}_j$ the phase rate per unit volume, $U_j$ the phase internal energy, $U_r$ the internal energy of rock, $h_j$ the phase enthalpy and $T$ the temperature. The thermal conduction coefficient $\kappa$ can be defined as

$$\kappa = \phi \sum_{j=1}^{n_p} s_j \kappa_j + (1-\phi)\kappa_r, \tag{3}$$

where $\kappa_j$ and $\kappa_r$ are the conduction coefficients of the fluid phases and the rock, respectively.

The fluid Darcy velocity $v_j$ considering gravity effects is defined as

$$\boldsymbol{v_j = K \frac{k_{rj}}{\mu_j} (\nabla p - \gamma_p \nabla D)}, \tag{4}$$

where $K$ is the permeability of the porous media, $k_{rj}$ the phase relative permeability, $\mu_j$ the phase viscosity, $p$ the pressure, $\gamma_p$ the specific weight, and $D$ the depth. The expression of porosity $\phi$ considering the rock compressibility is given by

$$\phi = \phi_0 \left(1 + c_r \left(p - p_{ref}\right)\right), \tag{5}$$

where $\phi_0$ is the initial porosity of the rock, $c_r$ the rock compressibility, and $p_{ref}$ the reference pressure.

In many geothermal systems, we can assume that only the water component is present which allows us to use pressure and enthalpy as primary variables (Khait & Voskov, 2018; Wang et al., 2020). These variables, encapsulated as state variables $\omega$, become the focus for solving the governing equations (eq. (1) and eq. (2)) using the Newton–Raphson method:

$$\frac{\partial g(\omega_k)}{\partial \omega_k} (\omega_{k+1} - \omega_k) = -g(\omega_k) \tag{6}$$

Here, $g$ represents the residual form of the governing equations, and the subscript $k$ specifies the $k^{th}$ nonlinear iteration. To handle well treatment and linearize eq. (1) and eq. (2), Operator-Based Linearization is employed (Khait & Voskov, 2018; Voskov, 2017).

## 3. FIRST RESULTS OF DIGITAL TWIN APPLICATION

The Delft campus geothermal well is used for extracting subsurface heat for the campus buildings and parts of the Delft city. This heat extraction process is subject to significant uncertainties, stemming from both operational and geological factors. The injection well Bottom Hole Pressure (BHP) forms an operational uncertainty and is dictated by geological uncertainties such as facies and porosities of the reservoir formation. The injection well BHP is largely influenced by the discharge rate and the connection between the injection and production well. The production well's trajectory log data is employed to assess the connection in the vicinity of the production well, thus constraining the geological models and uncertainties.

### 3.1 Reservoir model

The full geological model (Reinhard, 2019) was created in the past using data collected from the existing geothermal wells located in the West Netherlands Basin. The complete geological model consists of circa 38 million cells. Previous studies (Major et al., 2023; Wang et al., 2021) show the thermal response of a single active doublet in a large geothermal model will not be influenced by the size of the geological model. Therefore, a cropped geological model which consists of circa 5 million cells is used to study the thermal response. Figure 2 shows the full geological model and the cropped geological model with the injection and the production wells.

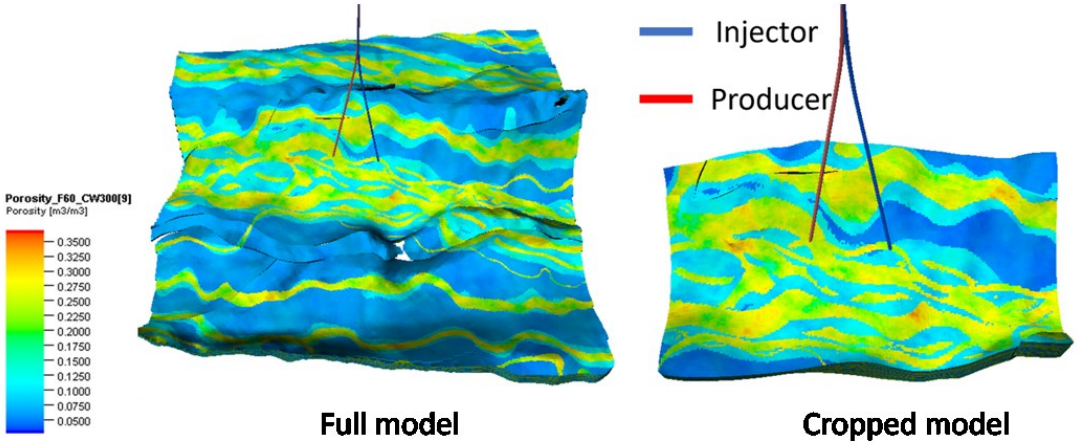


**Figure 2: The porosity distribution of full geological model and cropper simulation model**

The Lorenz coefficient is used to assess the degree of heterogeneity in the geological models. The Lorenz coefficient is calculated based on the Lorenz curve which is the relationship between normalized storage capacity and normalized flow capacity shown below

$$C_\phi = \frac{\sum(\phi h)_i}{\sum(\phi h)_t} \quad C_k = \frac{\sum(kh)_i}{\sum(kh)_t} \tag{7}$$

Based on these definitions, the Lorenz coefficient is calculated for representative geological realizations shown in fig. 3(a). The production well trajectory log data is introduced as a soft constraint on existing geological models. The porosity and permeability data collected from the well logs are plotted in fig. 3(b) together with other porosity/permeability correlations existing in the literature for the West Netherlands Basin. The correlation from Willems et al. (2020) based on the Delft Sandstone is the most consistent with the raw data points and is used for further investigations.

The porosities, extracted from the log data, are upscaled to the model resolution and compared with the model porosities along the production well trajectory for each realization. The MSE of porosity difference is computed for 870 existing geological realizations that were not originally constrained to the newly drilled well. A small ensemble of 18 realizations that have good alignment with the reference porosity is selected by applying 30%

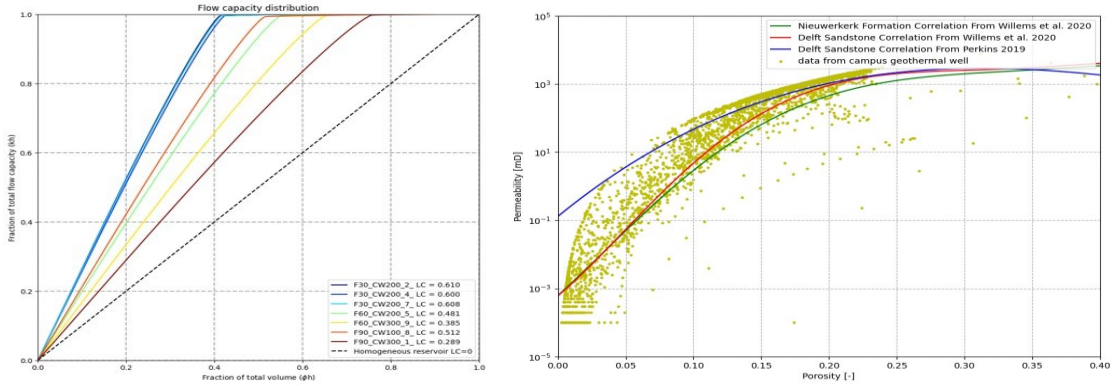


(a) Real Lorenz curve (b) Poro-perm correlation

**Figure 3: Lorenz curves for representative realizations (a) and porosity/permeability correlations with real data points based on uncorrected log data.**

of the maximum MSE cutoff on ascended MSE. Figure 4 shows the permeability and porosity distribution of 3 representative realizations out of 18 picked.

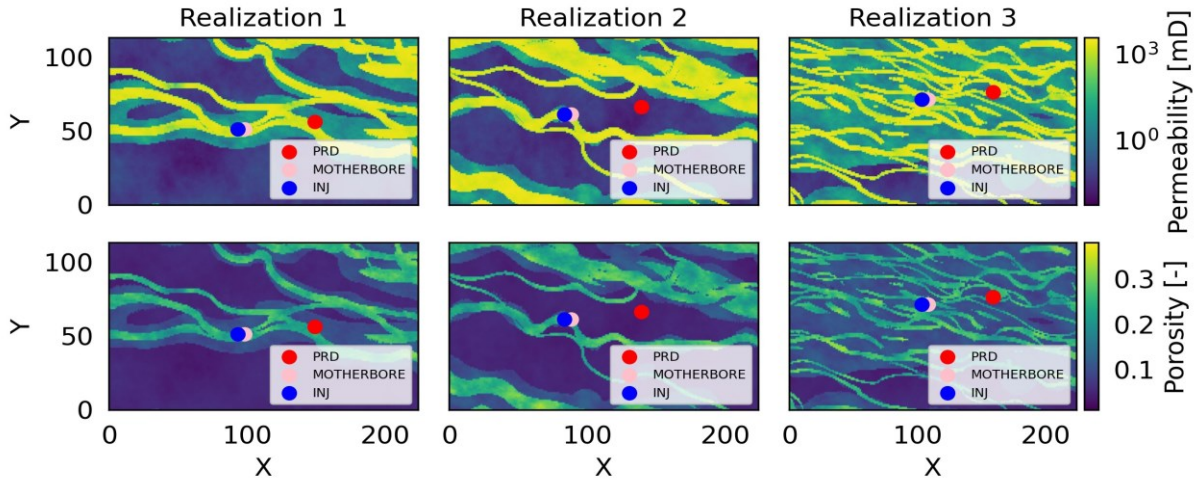


**Figure 4: 2D permeability (top row) and porosity (bottom row) distribution of three constrained representative realizations. Permeability is calculated based on the porosity-permeability correlation from Willems et al. (2020)**

Table 1 describes the major parameters used for the models below. We used the geological model resolution, especially in the vertical direction to preserve the accuracy of the model. Initial distribution of pressure and temperature is following the natural gradient. Besides, we designate properties of sandstone and shale in the model.

**Table 1: Parameter settings for reservoir model**

| Parameter | Value |
|---|---|
| Grid dimension | 224 × 113 × 200 |
| Grid size, m | 20 × 21 × (0.21 − 1.37) |
| Permeability, mD | (0.004–1113) |
| Porosity, - | (0.01–0.264) |
| Sandstone heat capacity, kJ/m$^3$/K | 2450 |
| Sandstone heat conductivity, kJ/m/day/K | 259.2 |
| Shale heat capacity, kJ/m$^3$/K | 2300 |
| Shale heat conductivity, kJ/m/day/K | 190.08 |
| Injection temperature, K | 298.15 |
| Injection/production rate, m$^3$/day | 8400 |

### 3.2 Effect of Heterogeneity to Injection Pressure

We consider the processed ensemble with 18 geological realizations, each of them containing more than 6 million control volumes. The production temperature and injection well Bottom Hole Pressure (BHP) (right) are shown in fig. 5. If the temperature technical limit is set to 350 K, the lifetime of the project varies by more than 20 years

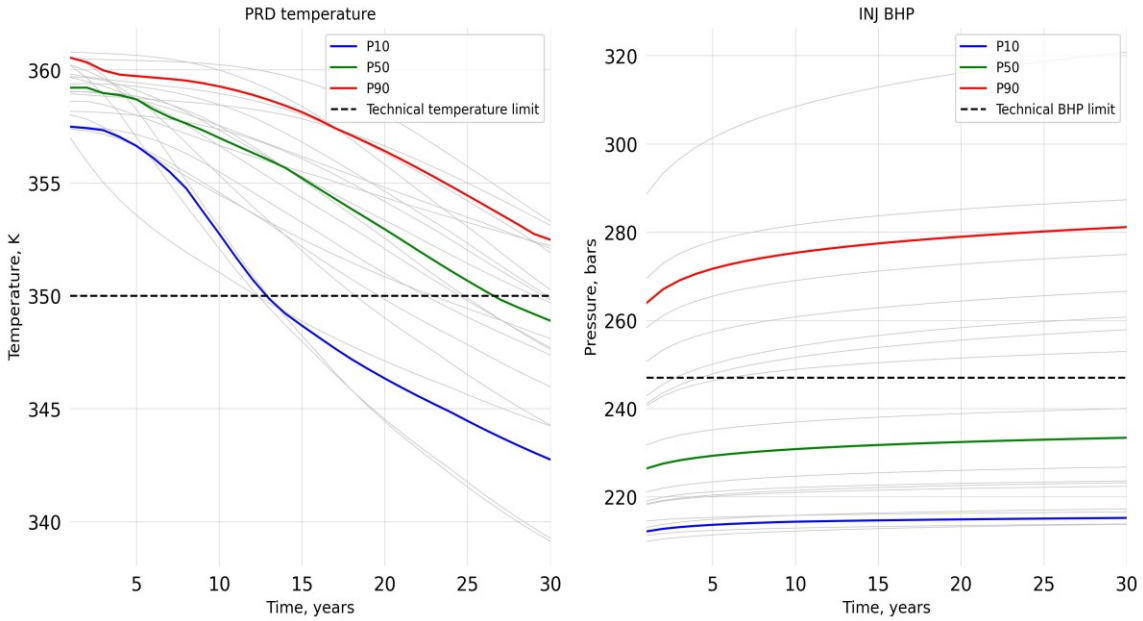


**Figure 5: Production temperature (a) and injection pressure (b) for the ensemble of 18 realizations**

between realizations. Following the Netherlands regulations, SodM and TNO (2013) define the maximum injection well BHP for a geothermal system as

$$BHP_{\max} = P_{\mathbf{reservoir}} + 0.0135 \times TVD_{\text{reservoir}}. \tag{8}$$

The protocol considers an average pressure gradient with depth as the upper boundary for injection pressure, without considering the in-situ stress under which the doublet operates. The maximum injection well BHP calculated based on these regulations is 247 bar. More than half of the realizations have BHP lower than SodM regulations. However, there are 7 realizations above the threshold. Characterizing the in-situ stresses via measurements could be used to inform a more comprehensive upper injection pressure limit. If stresses support increasing the injection BHP limits in a safe way, higher energy and economic output can be achieved (Daniilidis et al., 2020).

### 3.3 Evaluation of water loss in the abandoned well

Due to drilling challenges, the original injection well was lost due to instability, and the abandoned borehole was cemented at 1300 m True Vertical Depth (TVD) only, i.e. well above the cap-rock. Below this depth, the lost wellbore remains, possibly as an open hole section called 'motherbore' in the discussion below. The formations directly above the reservoir are expected to have some permeability. Another injection well is drilled sidetracking the initial bore, 100 m further. We investigate how much water could be lost to the layers above the reservoir section via the open-hole motherbore due to elevated pressure following injection from the sidetrack. Figure 6 is a schematic cross-section showing the configuration of the reservoir, the layers above the reservoir, and the wells. For simplicity and due to lack of data, we assume that the shape and properties of the open hole section in the motherbore do not change over time.

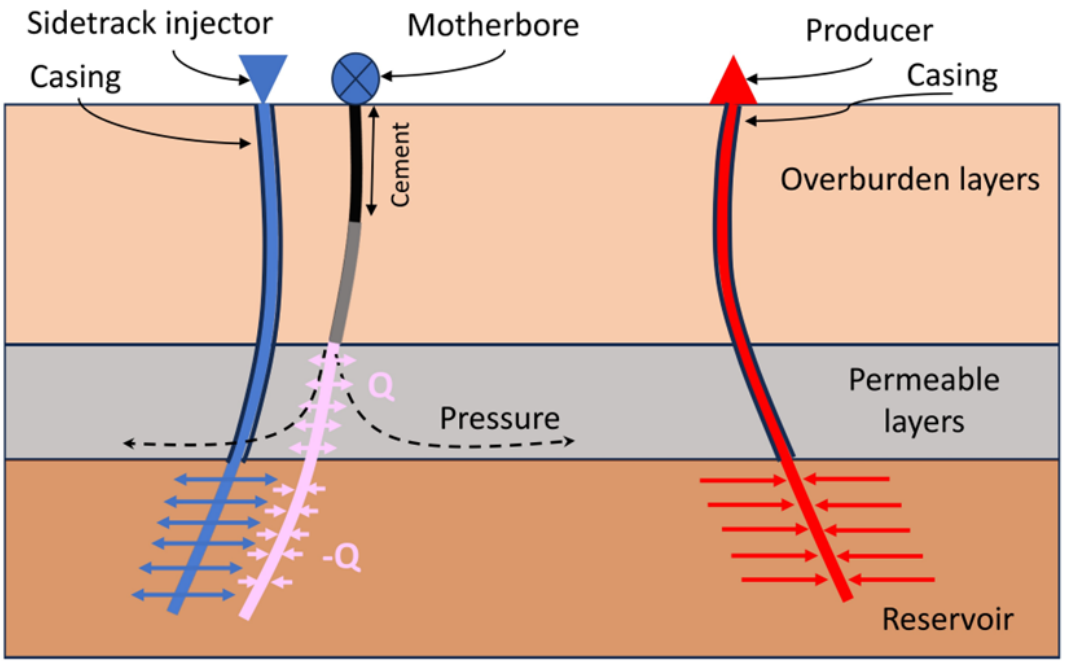


**Figure 6: Schematic view of the sidetrack well, the motehrbore (original injection well) and the production well. The grey section of the motherbore is assumed inactive and the pink part is assumed to be hydraulically connected to the reservoir.**

A simplified steady-state radial flow is applied to evaluate the water production rate for the layers above the reservoir. The steady-state model is coupled to the reservoir simulation model as described in section 3.1. The relationship between BHP and the water flow rate in the motherbore is:

$$p_{\mathrm{r}} - p_{\mathrm{w}} = \frac{q_{\mathrm{sc}} B \mu}{2\pi k h} \ln(r_{\mathrm{e}}/r_{\mathrm{w}} + s) \tag{9}$$

where $p_r$ and $p_w$ are reservoir pressure [Pa] and bottom-hole pressure [Pa] respectively, $q_{sc}$ flow rate at surface conditions [$m^3$/s], $B$ the fluid compressibility [$m^3/m^3$], $\mu$ fluid viscosity [Pa · s], $k$ matrix permeability [$m^2$], $h$ the thickness of the reservoir layer, $r_e$ reservoir radius [m], $r_w$ wellbore radius [m] and $s$ skin factor [-]. Notice, that this analytical formula is written under simplifying assumptions that the permeable reservoir above the target reservoir is infinite and the pressure pr in the reservoir is not changing with time.

We start the simulation from rate $Q = 0$. Based on BHP computed by the reservoir simulation for the first time step, we re-evaluate the rate and use it for the same time step in the analytical solution above. After a few iterations, the pressure is converged, and we use the same rate as an initial guess for the next time step. This procedure converges very quickly for the first few time steps and needs to be applied occasionally when the injection rate is changing. Rate changes can occur due to the cooling of a larger reservoir region when constant rate control is applied or when the rate control is significantly changing.

We evaluate the rate for the upper layers using parameters from the table 1 for reservoir simulation. The results are shown in section 3.2. Since the parameters of the upper layers are not well characterized, we consider the uncertainty in the parameters for these layers as discussed in literature Willems et al., 2020. The average thickness of the layer above the reservoir is derived from the well log in Willems et al., 2020 as around 90 m. The main parameter influencing the production rate in the upper layers is permeability and we took the endpoints of an average permeability range which lay between 200 to 810 mD in the study.

The well test in the production well evaluated the skin for production and injection wells around $s = 2.3$ which we used in the simulation. For the motherbore, we assumed the skin $s = 4.0$ since the wellbore is generally unstable and may collapse at certain intervals. Here, we only include the first of the permeable layers above the reservoir assuming that the connectivity with the rest of the layers along the wellbore is limited.

The ordered distribution of maximum and minimum total water production to the layers is evaluated for all 18 geological realizations and is shown in fig. 7. Depending on permeability distribution in the production interval, the water loss rate to the top layers varies between 150 to 2800 $m^3$/day. At the same time, (a), (b), and (c) in fig. 7 demonstrate the top view of permeability distribution from representative geological realizations, where we get minimum, median and maximum average water losses to the layers above the reservoir.

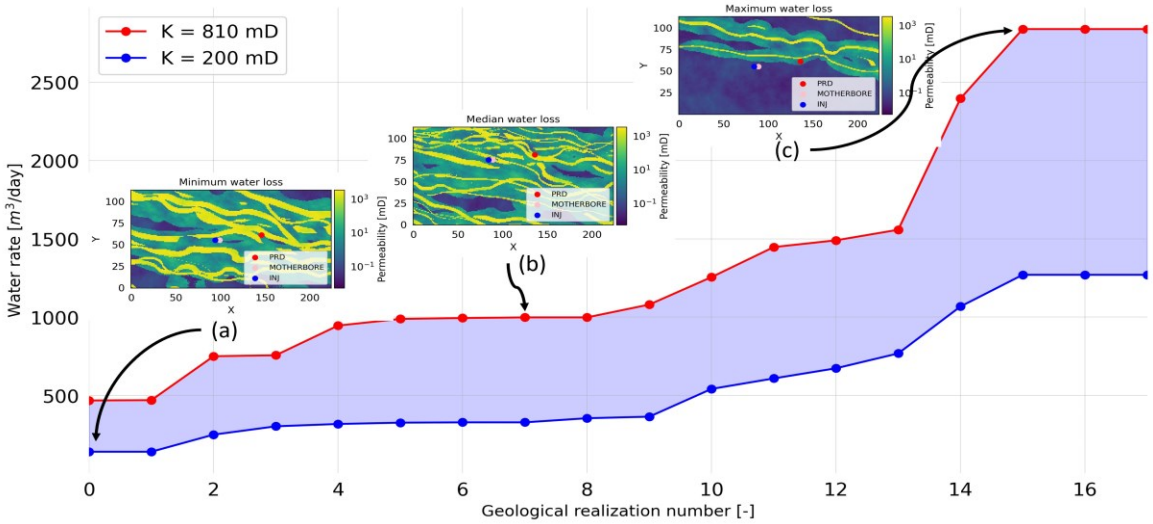


**Figure 7: The maximum and minimum average water losses to the layers above the reservoir and top view of representative realizations**

## 4. CONCLUSIONS AND DISCUSSION

In this study, we describe the concept of a digital twin for the geothermal project at the TU Delft campus. The open-source software RRM and DARTS, as the key parts of the above framework, are introduced. The results of two applications are discussed as follows:

We analyzed the high-fidelity geological models developed before wells were drilled and proposed the procedure of constraining them to the received well-log data. Subsequently, the constrained ensemble of models is employed to perform uncertainty analysis and estimate the risk of operating at Bottom Hole Pressure (BHP) above the regulation limits. Out of 18 realizations constrained to the well logs, 7 have predicted BHP higher than allowed by regulation. Further evaluation of stress distribution in the reservoir could result in a higher regulation limit.

Another investigation is related to the collapsed wellbore of the original injection well we call the motherbore. This motherbore is cemented up to 1300 m of TVD and part of it is assumed to connect the reservoir to the permeable layers above. Due to injection operation in the vicinity of the sidetrack injector, the cold water could flow through the motherbore to the upper permeable layers and cool down a larger column of rock than expected from injection to the reservoir only. To evaluate this effect, we proposed a semi-analytic model where inflow to the upper layers is evaluated based on the radial inflow within simplifying assumptions. This inflow model is coupled with a high-fidelity simulation of the geothermal reservoir in an iterative manner. Using the same ensemble, we evaluate the risk of water injection to the upper layers through the motherbore. Simulation results show the range of water loss to the upper layers between 150 to 2800 $m^3$/day for a target rate of injection at 8400 $m^3$/day. The water loss ratio ranges from 1.79% to 33.33%. In the presence of a high-permeability fault, water loss could potentially increase significantly.

In future work, we would like to improve the current geological models using the well logs, well tests, and other measured data. In addition to these improvements, a better geological understanding of the layers above the reservoir will refine the estimation of water loss to the upper layers. Next, a semi-analytical model will be employed to estimate the cold front propagation in the upper layers. After we obtain the temperature distribution of the top layers, we will investigate the potential risks associated with the cooling down of the larger formation volume. Besides, a proof-of-concept study for a doublet system will be conducted within the proposed digital twin workflow of subsurface geothermal production.

## REFERENCES

Alshakri, J., Hampson, G. J., Jacquemyn, C., Jackson, M. D., Petrovskyy, D., Geiger, S., Machado Silva, J. D., Judice, S., Rahman, F., & Costa Sousa, M. (2023). A screening assessment of the impact of sedimentological heterogeneity on $CO_2$ migration and stratigraphic-baffling potential: Sherwood and Bunter sandstones, UK.

*Geological Society, London, Special Publications*, *528*(1), 245–266. https://doi.org/10.1144/SP528-2022-34 Anderson, A., & Rezaie, B. (2019). Geothermal technology: Trends and potential role in a sustainable future [ISBN: 0306-2619 Publisher: Elsevier]. *Applied Energy*, *248*, 18–34.

Athens, N., & Caers, J. (2019). A monte carlo-based framework for assessing the value of information and development risk in geothermal exploration. *Applied Energy*, *256*, 113932. https://doi.org/10.1016/j.apenergy. 2019.113932

Baird, K., Geiger, S., Arnold, D., Doster, F., Hampson, G. J., Jacquemyn, C., Jackson, M. D., Petrovskyy, D., Geiger, S., Silva, J. D. M., Judice, S., Rahman, F., & Sousa, M. C. (2023). Assessing the impact of hierarchical geological heterogeneities on geothermal energy production [doi:10.3997/2214-4609.2023101116].

*84th EAGE Annual Conference and Exhibition*, 5.

Bentley, M. (2016). Modelling for comfort? [ISBN: 2041-496X Publisher: EAGE/Geological Society of London].

Bruhn, D. F., Wolf, K., Woning, M., Dalen, E. V., Nick, H. M., & Willems, C. J. L. (2015). The Delft Aardwarmte Project (DAP): Providing renewable heat for the university campus and a research base for the geothermal community. *World Geotherm. Congr*.

Brunetti, C., Bianchi, M., Pirot, G., & Linde, N. (2019). Hydrogeological model selection among complex spatial priors [ISBN: 0043-1397 Publisher: Wiley Online Library]. *Water Resources Research*, *55*(8), 6729–6753.

Chang, D., J., H., M., C., & S., C. (1994). Effective porosity, producible fluid and permeability in carbonates from nmr logging. *SPWLA 35th Annual Logging Symposium*.

Chen, Y. (2017). Integrated and intelligent manufacturing: Perspectives and enablers [ISBN: 2095-8099 Publisher: Elsevier]. *Engineering*, *3*(5), 588–595.

Daniilidis, A., Alpsoy, B., & Herber, R. (2017). Impact of technical and economic uncertainties on the economic performance of a deep geothermal heat system. *Renewable Energy*, *114*, 805–816. https://doi.org/10.1016/ j.renene.2017.07.090

Daniilidis, A., Khait, M., Saeid, S., Vokov, D., & Bruhn, D. (2020). A high performance framework for the optimization of geothermal systems, comparing energy production and economic output. *Proceedings World Geothermal Congress 2020*, 491–515. https://pangea.stanford.edu/ERE/db/WGC/papers/WGC/2020/33047.pdf

Daniilidis, A., Nick, H., & Bruhn, D. (2021). Interference between geothermal doublets across a fault under subsur-

face uncertainty; implications for field development and regulation. *Geothermics*, *91*, 1–13.

De Paepe, M., & Mertens, D. (2007). Combined heat and power in a liberalised energy market. *Energy Conversion and Management*, *48*, 2542–2555. https://doi.org/10.1016/j.enconman.2007.03.019

Glaessgen, E., & Stargel, D. (2012). The digital twin paradigm for future NASA and US Air Force vehicles. *53rd AIAA/ASME/ASCE/AHS/ASC structures, structural dynamics and materials conference 20th AIAA/ASME/AHS adaptive structures conference 14th AIAA*, 1818.

Grieves, M. (2014). Digital twin: Manufacturing excellence through virtual factory replication. *White paper*, *1*(2014), 1–7.

Hoteit, I., Luo, X., & Pham, D.-T. (2012). Particle kalman filtering: A nonlinear bayesian framework for ensemble kalman filters. *Monthly Weather Review*, *140*(2), 528–542. https://doi.org/10.1175/2011mwr3640.1

Jackson, M. D., Hampson, G. J., & Sech, R. P. (2009). Three-dimensional modeling of a shoreface-shelf parasequence reservoir analog: Part 2. Geologic controls on fluid flow and hydrocarbon recovery [ISBN: 1558-9153 Publisher: American Association of Petroleum Geologists (AAPG)]. *AAPG bulletin*, *93*(9), 1183–1208.

Jackson, W. A., Hampson, G. J., Jacquemyn, C., Jackson, M. D., Petrovskyy, D., Geiger, S., Silva, J. D. M., Judice, S., Rahman, F., & Sousa, M. C. (2022). A screening assessment of the impact of sedimentological heterogeneity on CO2 migration and stratigraphic-baffling potential: Johansen and Cook formations, Northern Lights project, offshore Norway [ISBN: 1750-5836 Publisher: Elsevier]. *International Journal of Greenhouse Gas Control*, *120*, 103762.

Jacquemyn, C., Hossain, S., Jackson, W. A., Alshakri, J., Hampson, G. J., Jackson, M. D., Petrovskyy, D., Baird, K., Geiger, S., & Silva, J. M. (2023). Sketch-based modelling with flow diagnostics: Prototyping geomodels for better resource modelling decisions [Issue: 1]. *84th EAGE Annual Conference & Exhibition*, *2023*, 1–5.

Jacquemyn, C., Jackson, M. D., & Hampson, G. J. (2019). Surface-based geological reservoir modelling using gridfree NURBS curves and surfaces [ISBN: 1874-8961 Publisher: Springer]. *Mathematical Geosciences*, *51*, 1– 28.

Jacquemyn, C., Pataki, M. E. H., Hampson, G. J., Jackson, M. D., Petrovskyy, D., Geiger, S., Marques, C. C., Machado Silva, J. D., Judice, S., Rahman, F., & Costa Sousa, M. (2021). Sketch-based interface and modelling of stratigraphy and structure in three dimensions. *Journal of the Geological Society*, *178*(4), jgs2020–187. https://doi.org/10.1144/jgs2020-187

Jolie, E., Scott, S., Faulds, J., Chambefort, I., Axelsson, G., Guti´errez-Negr´ın, L. C., Regenspurg, S., Ziegler, M., Ayling, B., & Richter, A. (2021). Geological controls on geothermal resources for power generation [ISBN:

2662-138X Publisher: Nature Publishing Group UK London]. *Nature Reviews Earth & Environment*, *2*(5), 324–339.

Khait, M., & Voskov, D. (2018). Operator-based linearization for efficient modeling of geothermal processes. *Geothermics*, *74*, 7–18.

Konstantopoulos, I., Siratovich, P., Buster, G., Taverna, N., Weers, J., Blair, A., Huggins, J., Siega, C., Mannington, W., Urgel, A., Cen, J., Quinao, J., Watt, R., & Akerley, J. (2023). Deploying Digital Twins for Geothermal Operations with the GOOML Framework. *48th Workshop on Geothermal Reservoir Engineering*.

Linde, N., Renard, P., Mukerji, T., & Caers, J. (2015). Geological realism in hydrogeological and geophysical inverse modeling: A review [ISBN: 0309-1708 Publisher: Elsevier]. *Advances in Water Resources*, *86*, 86–101.

Lund, J. W., & Toth, A. N. (2021). Direct utilization of geothermal energy 2020 worldwide review [ISBN: 0375-6505 Publisher: Elsevier]. *Geothermics*, *90*, 101915.

Major, M., Daniilidis, A., Hansen, T. M., Khait, M., & Voskov, D. (2023). Influence of process-based, stochastic and deterministic methods for representing heterogeneity in fluvial geothermal systems. *Geothermics*, *109*. https://doi.org/10.1016/j.geothermics.2023.102651

Oliver, D. S., Reynolds, A. C., & Liu, N. (2008). *Inverse theory for petroleum reservoir characterization and history matching*. Cambridge University Press. https://doi.org/10.1017/cbo9780511535642

Osinde, N. O., Byiringiro, J. B., Gichane, M. M., & Smajic, H. (2019). Process modelling of geothermal drilling system using digital twin for real-time monitoring and control [ISBN: 2411-9660 Publisher: MDPI]. *Designs*, *3*(3), 45.

O'Sullivan, M., & O'Sullivan, J. (2016). Reservoir modeling and simulation for geothermal resource characterization and evaluation. In *Geothermal power generation* (pp. 165–199). Elsevier. https://doi.org/10.1016/b978-008-100337-4.00007-3

Petrovskyy, D., Jacquemyn, C., Geiger, S., Jackson, M. D., Hampson, G. J., Silva, J. M., Judice, S., Rahman, F., & Sousa, M. C. (2023). Rapid flow diagnostics for prototyping of reservoir concepts and models for subsurface CO2 storage [ISBN: 1750-5836 Publisher: Elsevier]. *International Journal of Greenhouse Gas Control*, *124*, 103855.

Rath, V., Wolf, A., & Bu¨cker, H. M. (2006). Joint three-dimensional inversion of coupled groundwater flow and heat transfer based on automatic differentiation: Sensitivity calculation, verification, and synthetic examples. *Geophysical Journal International*, *167*(1), 453–466. https://doi.org/10.1111/j.1365-246x.2006.03074.x

Refsgaard, J. C., Christensen, S., Sonnenborg, T. O., Seifert, D., Højberg, A. L., & Troldborg, L. (2012). Review of strategies for handling geological uncertainty in groundwater flow and transport modeling [ISBN: 0309-1708 Publisher: Elsevier]. *Advances in Water Resources*, *36*, 36–50.

Reinhard, P. (2019). *Pressure and Temperature Interference for Geothermal Projects in Dense Production Areas A Case Study for the Delft Area* [Master's Thesis]. Delft University of Technology.

SodM & TNO. (2013). Protocol injectiedrukken bij aardwarmte.

Tian, X., Volkov, O., & Voskov, D. (2024). An advanced inverse modeling framework for efficient and flexible adjointbased history matching of geothermal fields. *Geothermics*, *116*. https://doi.org/10.1016/j.geothermics. 2023.102849

Vardon, P., Bruhn, D., Steiginga, A., Cox, B., Abels, H., Barnhoorn, A., Drijkoningen, G., Slob, E., & Wapenaar, K. (2020). A Geothermal Well Doublet for Research and Heat Supply of the TU Delft Campus. *arXiv preprint arXiv:2003.11826*.

Vardon, P. J., Abels, H. A., Barnhoorn, A., Daniilidis, A., Bruhn, D., Drijkoningen, G., Elliott, K., van Esser, B., Laumann, S., van Paassen, P., Vargas-Meleza, L., Vondrak, A., & Voskov, D. (2024). A research and energy production geothermal project on the tu delft campus: Project implementation and initial data collection. *Proceedings Stanford Geothermal Workshop 2024*.

Voskov, D. V. (2017). Operator-based linearization approach for modeling of multiphase multi-component flow in porous media. *Journal of Computational Physics*, *337*, 275–288.

Wang, Y., Voskov, D., Khait, M., & Bruhn, D. (2020). An efficient numerical simulator for geothermal simulation: A benchmark study. *Applied Energy*, *264*. https://doi.org/10.1016/j.apenergy.2020.114693

Wang, Y., Voskov, D., Daniilidis, A., Khait, M., Saeid, S., & Bruhn, D. (2023). Uncertainty quantification in a heterogeneous fluvial sandstone reservoir using gpu-based monte carlo simulation. *Geothermics*, *114*. https://doi.org/10.1016/j.geothermics.2023.102773

Wang, Y., Voskov, D., Khait, M., Saeid, S., & Bruhn, D. (2021). Influential factors on the development of a lowenthalpy geothermal reservoir: A sensitivity study of a realistic field. *Renewable Energy*, *179*, 641–651. https://doi.org/10.1016/j.renene.2021.07.017

Willems, C., Vondrak, A., Mijnlieff, H., Donselaar, M., & van Kempen, B. (2020). Geology of the Upper Jurassic to Lower Cretaceous geothermal aquifers in the West Netherlands Basin – an overview. *Netherlands Journal of Geosciences*, *99*, 1–13.

Wu, H., Fu, P., Hawkins, A. J., Tang, H., & Morris, J. P. (2021). Predicting thermal performance of an enhanced geothermal system from tracer tests in a data assimilation framework. *Water Resources Research*, *57*(12). https://doi.org/10.1029/2021wr030987

Yousefzadeh, R., Kazemi, A., Ahmadi, M., & Gholinezhad, J. (2023). Geological Uncertainty Quantification. In *Introduction to Geological Uncertainty Management in Reservoir Characterization and Optimization: Robust Optimization and History Matching* (pp. 15–42). Springer.

Yu, W., Patros, P., Young, B., Klinac, E., & Walmsley, T. G. (2022). Energy digital twin technology for industrial energy management: Classification, challenges and future [ISBN: 1364-0321 Publisher: Elsevier]. *Renewable and Sustainable Energy Reviews*, *161*, 112407.

Zhang, Z., Jafarpour, B., & Li, L. (2014). Inference of permeability heterogeneity from joint inversion of transient flow and temperature data. *Water Resources Research*, *50*(6), 4710–4725. https://doi.org/10.1002/ 2013wr013801